GEOMATICS AND ENVIRONMENTAL ENGINEERING • Volume 17 • Number 5 • 2023

https://doi.org/10.7494/geom.2023.17.5.61

Nevil Wickramathilaka[1], Uznir Ujang[2], Suhaibah Azri[3], Tan Liat Choon[4]

Calculation of Road Traffic Noise, Development of Data, and Spatial Interpolations for Traffic Noise Visualization in Three-dimensional Space

Abstract: Road traffic noise visualization is vital in three-dimensional (3D) space. Designing noise observation points (NOPs) and the developments of spatial interpolations are key elements for the visualization of traffic noise in 3D. Moreover, calculating road traffic noise levels by means of a standard noise model is vital. This study elaborates on the developments of data and spatial interpolations in 3D noise visualization. In 3D spatial interpolation, the value is interpolated in both horizontal and vertical directions. Eliminating flat triangles is vital in the vertical direction. Inverse distance weighted (IDW), kriging, and triangular irregular network (TIN) are widely used to interpolate noise levels. Because these interpolations directly support the interpolation of three parameters, the developments of spatial interpolations should be applied to interpolate noise levels in 3D. The TIN noise contours are primed to visualize traffic noise levels while IDW and kriging provide irregular contours. Further, this study has identified that the TIN noise contours fit exactly with NOPs in 3D. Moreover, advanced kriging interpolation such as empirical Bayesian kriging (EBK) also provides irregular shape contours and this study develops a comparison for such contours. The 3D kriging in EBK provides a significant approach to interpolate noise in 3D. The 3D kriging voxels show a higher accurate visualization than TIN noise contours.

Keywords: spatial interpolation, 3D, IDW, kriging, EBK, 3D kriging, spatial developments

Received: 4 March 2023; accepted: 1 July 2023

[1] Universiti Teknologi Malaysia, Faculty of Built Environment and Surveying, Johor, Malaysia, email: nevilvidyamanee@kdu.ac.lk (corresponding author), https://orcid.org/0009-0003-9772-0070
[2] Universiti Teknologi Malaysia, Faculty of Built Environment and Surveying, Johor, Malaysia, email: mduznir@utm.my, https://orcid.org/0000-0001-5281-8478
[3] Universiti Teknologi Malaysia, Faculty of Built Environment and Surveying, Johor, Malaysia, email: suhaibah@utm.my, https://orcid.org/0000-0001-7926-9608
[4] Universiti Teknologi Malaysia, Faculty of Built Environment and Surveying, Johor, Malaysia, email: tlchoon@utm.my, https://orcid.org/0000-0002-1548-3098

1. Introduction

Road traffic noise pollution is a serious environmental problem and identifying road traffic noise pollution through a 3D visualization is vital.

1.1. Road Traffic Noise and Visualization

Not all sound is considered to be noise pollution. The World Health Organization (WHO) has identified noise above 55 dB as a possible health hazard and has concluded that people should not be exposed to such levels [1, 2], but this limitation depends on the country. According to the emission of road traffic noise:, the noise limitation level in Malaysia is 55 dB during the day time and 50 dB for night time; Germany has levels of 45 dB during the day and 35 dB for night time; Japan is 45 dB during the day time and 35 dB for night time; Iran is 55 dB during the day time and 45 dB for night; and Australia is 45 dB during the day time and 35 dB for night time [3]. The noise level generated by each vehicle to the noise receivers is a perpendicular propagation from the centerline of the road [4]. Noise propagation frequently happens through a line source in most urban cities. This assumption fails if the receiver points are located on the line source. A line traffic noise source is spread as cylindrical sound waves, and a point source spread spherical spreading from the particular vehicles [5].

Urbanization is one of the major drivers behind extensive noise pollution [6]. It is caused by the movement of vehicles such as automobiles, and road traffic noise pollution is 90% of noise pollution in urban areas [7]. Traffic noise can travel in every direction and heard from some distance away [8]. The three-dimensional (3D) visualization of noise provides an accurate representation so that people can identify the risks of noise pollution [9]. The road traffic noise visualization consists of a traffic noise calculation to noise observation points (NOPs), traffic noise interpolation, and visualization. Road traffic noise models are mathematical models that are used to measure and predict the vehicle noise. These models are used to assess the impact of traffic noise and to plan noise mitigation strategies [9, 10]. A suitable noise model is vital for accurate noise calculations [10]. One of the most common methods to visualize traffic noise is a combination of traffic noise surfaces and a 3D city model [11]. However, collecting road traffic noise levels from everywhere is an impossible task and thus calculating traffic noise levels to noise observation points by means of a noise model is crucial, together with spatial interpolation. In addition, reviewing spatial interpolations and their developments are also important. Unlike 2D visualization, developments of spatial interpolation are essential to interpolate traffic noise levels in 3D. The noise contours are lines or curves that represent the same noise level or sound pressure level both 2D and 3D [12]. In addition, raster cells are small squares or rectangles that are used to create a visual representation of the intensity of sound in a given area [13] and 3D noise contours and 3D voxels are primed to visualize traffic noise in 3D.

Road traffic noise models can be used to calculate noise levels along both vertical and horizontal propagation. The factors of road traffic noise calculation are not constants even in different cities of the same country. Therefore, several amendments to existing noise models are required for traffic noise calculations [14] and reviewing the standard road traffic noise model is vital to road traffic noise mapping. Sounds from engine noise, tire and road friction, road surface type, and rolling noise are the main contributors to the generation of traffic noise [15]. Furthermore, road traffic, human qualities [16], transportation networks, and environmental conditions all lead to increased traffic noise pollution [17]. Speed, volume, acceleration and deceleration, the volume of heavy vehicles, road gradients, noise reflection, and noise absorption by ground are further important factors in traffic noise pollution [18].

1.2. Road Traffic Noise Model

The Federal Highway Administration (FHWA) model consists of the following: vehicle distributions, traffic pattern, types of the surface of the buildings, the heights of the receiver, barriers, and the type of the pavements are considered as factors of traffic noise [19, 20]. Meanwhile, the RLS-90 model includes: average hourly traffic flow, number of vehicles such as motorcycles, light and heavy vehicles, and average vehicle speed of each group, type, and shape of the roads, barriers, and noise absorption are considered parameters [21, 22]. The CoRTN model is suitable for rush and free long line hour traffic situations, and where the vehicle spacing is inter-vehicular spacing is not more related to the distances or uneven. The speed of cars, the composition of the vehicles, the number of vehicles, the road's gradient, and the road surface condition are used to calculate the noise levels [22, 23].

Finally, we have the Henk de Kluijver noise model which considers the physical, natural, and traffic conditions. Moreover, this model is highly flexible and can be used for different types of environments. The number of vehicles, type of vehicles, speed of vehicles, noise reflection, noise absorb by ground, noise barriers, and weather conditions are the parameters of this model [9, 24]. Furthermore, this noise model has proceeded to calculate road traffic noise levels in a vertical direction around the buildings near the Hemmat highway in Iran [9]. Vertical propagation of traffic noise along the facades of buildings has been considered in this study. Moreover, 2D visualization of road traffic noise has been shown along the vertical direction. Furthermore, this study demonstrates several significant methods to design NOPs along both vertical and horizontal directions and methods of traffic noise visualization like noise contours, and raster visualization. Therefore, the Henk de Kluijver road traffic noise model has been selected for this study due to its greater number of traffic noise parameters.

1.3. Road Traffic Noise Propagation along Vertical Direction

The heights of the buildings affect road traffic noise differences in the vertical direction. The distance of the traffic noise propagation path between the noise source and receiver is vital for the noise difference [25]. Decreasing road traffic noise

levels between two NOPs is smaller in the vertical direction than in the horizontal direction and variations in traffic noise levels on lower floors are higher than on higher floors [26]. In road traffic noise propagation over the ground, there will be energy losses due to ground absorption. The ground effect is weaker for the higher stories than for the lower stories [25]. Furthermore, the ground effect loses acoustic energy up to a certain height. In addition, properties of air, such as humidity, temperature, and wind vary with positions of vertical direction. Therefore, inserting ground effect, noise absorption by air, and weather correction for the vertical propagation of road traffic noise is vital to increase the accuracy [25]. The shape of the facades of buildings affects changes in traffic noise levels in the vertical direction but it does not seem to contribute to traffic noise propagation in the horizontal [26].

1.4. Noise Observation Points (NOPs)

The 3D city noise model can be used to display the intensity of noise levels in a particular area. However, several studies have been conducted for 3D road traffic noise visualization, and two-dimensional (2D) visualization was widely used [27]. NOPs are used to measure the noise level in a specific location, and interpolation is used to predict the noise level in the surrounding areas [24]. The purpose of NOPs is to identify noise levels and their design is an important process [28]. NOPs are designed as grid patterns [24] and in 2D visualization, the x coordinate, the y coordinate, and the noise level of a NOPs are considered for interpolation. This means that three parameters of a noise observation point are considered for 2D interpolation [29]. In 3D interpolation, the noise values are interpolated in the vertical direction. When considering NOP in a 3D space, it has an x coordinate, a y coordinate, a z coordinate, and a noise level (four parameters) [30]. The overlap of NOPs should be eliminated along the vertical direction. It is denoted as avoiding flat triangles (different z values for the same x and y coordinates) in spatial interpolation [24]. The distance interval of NOPs impacts the accuracy of the interpolation [24]. The inverse distance weighted (IDW), kriging, and TIN spatial interpolation are widely used for noise interpolation [31]. The IDW, kriging, and TIN interpolations are directly supported for 2D noise interpolation [32]. However, developments in spatial interpolation are required for 3D road traffic noise interpolation [33]. The elements of spatial interpolation are vital. The weighting factor is 2 of the IDW, the Delaunay triangulation of the TIN, and the Gaussian variogram of the kriging enhance the accuracy of spatial interpolation [31, 34]. The 3D kriging in empirical Bayesian kriging is vital to interpolate road traffic noise levels in 3D space [35]. For 3D kriging, there is no need to design NOP as eliminating flat triangles, meaning that it not necessary to design NOPs in order to eliminate the same x and y coordinates for different z values on the same vertical axis [36]. The noise levels are interpolated as horizontal slices along the vertical direction in 3D kriging. Furthermore, the 3D voxel embedded with 3D kriging shows a significant noise visualization in 3D space [37].

1.5. Two-Dimensional Spatial Interpolation and Visualisation

The object or phenomenon moving along the vertical axis is not considered in 2D spatial interpolation. As an example, noise levels are not described on a vertical axis in 2D. The accuracy and comparison of elements of 2D spatial interpolation are vital. The IDW is a deterministic method for spatial interpolation and the weighted average of known points is considered [38, 39]. However, the correlation of neighborhood points is not considered [40]. It means that IDW is more effective in visualizing road traffic noise in undulated and obstacles areas. Because of these variations, road traffic noise is higher in these areas [31]. Equation (1) [41] shows that:

$$w(x,y) = \sum_{i=0}^{N} \lambda i wi \ , \ \lambda i = \frac{di^p}{\sum_{i=1}^{N} d_{ki}^p} \tag{1}$$

where:

$w(x, y)$ – the interpolated value positioned at the point (x, y),
ki – the weight of the known results,
wi – positioned at point (xi, yi),
N – the number of observed (known) points (x, y),
λi – the weight at the point i,
di – the distance between the observed (known) point (xi, yi) and the estimate point (x, y),
p – the weighting factor [42].

The influence of the weighting factor is vital for the smoothness and accuracy of the interpolated surface [43]. According to Equation (1), IDW can be used to interpolate three parameters easily. However, a NOP consists of four parameters (x coordinate, y coordinate, z coordinate, and a noise value) in a 3D space. Therefore, developments of spatial interpolations should be adopted for IDW to 3D spatial interpolation. When increasing the weighting factor, the interpolated value shows greater similarity to the value of known points [44]. Traffic noise is reduced by approximately 1 dB over a 2 m distance in noise propagation along the horizontal direction [9, 45]. Thus, there is a greater value difference in neighborhood points. Therefore, assigning a suitable value to the weighting factor is vital for road traffic noise interpolation [46].

Kriging is a geostatistical method [47]. Kriging is applicable for large-size and clustered data. Thus, if the observation points have a correlation, kriging is preferred [48] and the correlation of points is measured by semivariance [49]. The function of kriging is described in Equation (2) [44]:

$$Z(s_o) = \sum_{i=0}^{N} \lambda i z(si) \tag{2}$$

where:

s_o – the interpolated point,
$z(si)$ – the observed value (known point),
N – the number of observed (known) values,
λi – the weight of the observed points.

In kriging, the weight does not only depend on the inverse of distance like IDW but also the variogram [50]. The Gaussian variogram is vital to increase the accuracy of the traffic noise interpolation [51]. The studies show the accuracy comparison of IDW and kriging for 2D road traffic noise mapping [24, 31]. However, the results of this study can be embedded in 3D road traffic noise mapping since kriging is more effective in the interpolation of clustered data. This means that if the road traffic noise levels have smaller variations in comparison to neighboring noise levels, kriging is possible to interpolate [24]. The triangular irregular network (TIN) is not widely used for noise interpolation [52] but it is suitable for highly variable noise levels. TIN provides a vector-based triangulated surface and Delaunay triangulation is vital to interpolate traffic noise levels [34]. As mentioned above, IDW, kriging, and TIN spatial interpolations are vital to interpolate three parameters. This means that this interpolation can be easily used for the interpolation of 2D road traffic noise but developments of spatial interpolation should be adopted to interpolate road traffic noise in 3D.

1.6. Three-dimensional Interpolation and Voxel Visualization

The 3D data show that the value of points changes faster in the vertical direction than in the horizontal direction [53]. This means that environmental processes move slowly along the same height and the prediction of a new location of a point can be sought with respect to vertical and horizontal directions [54]. 3D kriging is effective for these situations. According to the Henk de Kluijver road traffic noise model, noise reduces by approximately 2 dB within 2 m during horizontal propagation. There is the same noise level for the same parallel line to the centerline of the road if there are no noise barriers, noise reflection, and noise absorption by ground. The same is true for the vertical direction, as the noise levels are the same for horizontal levels in the vertical direction. Thus, 3D kriging can be applied to interpolate road traffic noise levels from the facades of buildings. 3D kriging is a geostatistical interpolation technique that can be used to interpolate values from multiple observations [55]. 3D kriging is an empirical Bayesian kriging that can be used to interpolate three-dimensional data, such as noise levels at different heights [56]. The difference in how we observe changes of values vertically and horizontally is the elevation factor assigned. However, linear trends should be removed in the vertical direction (Fig. 1) [2]. The elevation factor is determined according to the stretching of the elevation of an observed point along the vertical axis while making the same horizontal coordinates [57]. This elevation factor allows us to find a correct variogram model, neighbors, and suitable weights. If the weighting factor is not applied before processing, it is automatically calculated in run time using the maximum likelihood method [58]. While the developments of interpolations do not need 3D kriging such as IDW, TIN, and kriging for 3D road traffic noise interpolation [59], 3D kriging is vital for interpolating points consisting of x and y coordinates, a height value, and an observed value (noise levels) [60]. The output of 3D kriging is a 3D geostatistical layer but this 3D layer can move along the vertical axis (see Fig. 2) [61].

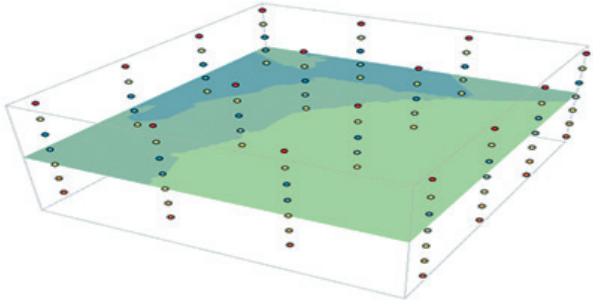

Fig. 1. Stretching of points
Source: [57]

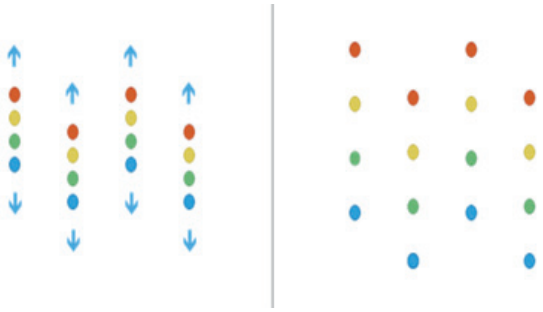

Fig. 2. 3D geostatistical layers
Source: [57]

A voxel is a three-dimensional pixel, and it looks like a three-dimensional grid forming a cube. Since road traffic noise travels in every direction, it has 3D view and thus 3D pixels are effective in representing road traffic noise in a 3D space. A voxel model is created for the data, which is interpolated on 2D slices. Selecting a well-defined 3D volume for the spatial distribution of input data denotes voxelization. A voxel shows the multidimensional spatial of 3D volumetric visualization [62]. The 3D kriging provides multidimensional voxel layers, including data captured at multiple depths [63, 64]. The formation of the voxels between the consecutive 3D kriging geostatistical layers is a significant process [65].

According to Figure 3, the information of the voxel can be filled under the positional relationship between the voxel and the layers. The type I voxel is completely removed, because any layer does not belong to the voxel. The type II voxel needs to be split, this type of voxel passed through a layer and, therefore, it needs to be split [65]. The type III voxel is needed to complete retention, because these voxels exist between the two layers. Thus, 3D kriging road traffic noise geostatistical layers along the vertical direction can be embedded in 3D voxels to represent road traffic noise in a 3D space via 3D kriging.

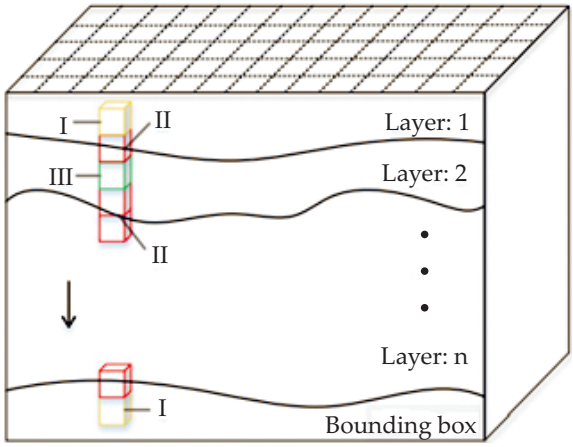

Fig. 3. Voxel and the 3D geostatistical layer
Source: [65]

2. Methodology

Calculating road traffic noise, spatial interpolation, and developments are essential for the 3D representation of road traffic noise levels. To further improve the quality of road traffic noise visualization, the data generation and accuracy comparison of spatial interpolation are vital.

2.1. Study Area

The study area is the Centre for Environmental and Sustainability, located at the Universiti Teknologi Malaysia (UTM), Johor, Malaysia. The location is 1°33′39.2″N 103°38′13.48″E. There is higher traffic noise in the morning and evening due to higher traffic flows. This study was carried out to visualize the traffic noise of six building facades and around the buildings in 3D. The Henk de Kluijver road traffic noise model was used to calculate traffic noise levels along a vertical direction. This research was conducted as model research to prepare traffic noise control strategies for UTM. Moreover, this study shows a comparison of accuracy, IDW, TIN, kriging, and 3D kriging for interpolating traffic noise via noise contours and raster noise voxels. Figure 4 illustrates the overview of the study area.

To visualize traffic noise in a 3D space, the visualization of traffic noise should be embedded with a 3D building model (see Fig. 7). The building model of this study was created using drone survey and GIS approaches. The level of details (LoD1) model was used for building information modelling (BIM). There are no curved facades of buildings, and all the facades are flat. Calculating traffic noise levels to NOPs is vital and are designed in the horizontal and vertical axes. The Henk de Kluijver traffic noise model was used to calculate traffic noise levels.

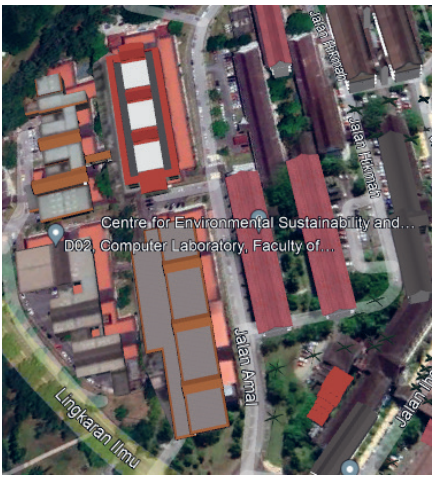

Fig. 4. Overview of the study area
Source: Google Earth

The Henk de Kluijver traffic noise model is shown in Equation (3) [9]:

$$L_{Aeq} = E + C_{\text{optrek}} + C_{\text{reflectie}} - D_{\text{afstand}} - D_{\text{lucht}} - D_{\text{bodem}} - D_{\text{meteo}} - D_{\text{barrier}} \quad (3)$$

where:

L_{Aeq} – the average noise level,
E – the level of noise emission,
C_{optrek} – the extra noise emission from braking and accelerating,
$C_{\text{reflectie}}$ – the noise reflection of buildings and barriers,
D_{afstand} – the reduction of traffic noise with distance,
D_{lucht} – the absorption of noise from the air,
D_{bodem} – the traffic noise absorption by the ground,
D_{meteo} – the mitigation of noise caused by wind conditions,
D_{barrier} – the construction of wall barriers alongside highways to reduce noise (the obstacles alter the real path of road traffic noise propagation; as a result, there is a significant loss in noise intensity).

Figure 5 shows the research workflow of the study.

According to the Henk de Kluijver traffic model, traffic noise depends on road statistical data (speed of vehicles, type of vehicles, and number of vehicles), noise absorption by ground, noise reflection by buildings, and barriers on the opposite side of the road. The numbers of vehicles were collected manually from 7.30 a.m. to 9.30 a.m. There is a higher traffic flow during this time. Furthermore, light, medium, and heavy vehicles were considered to collect the total number of vehicles. These data were collected for three weeks. The L_{Aeq} is the average road traffic noise level for a day. In this study, the time duration was limited to 7.30 a.m. to 9.30 a.m.

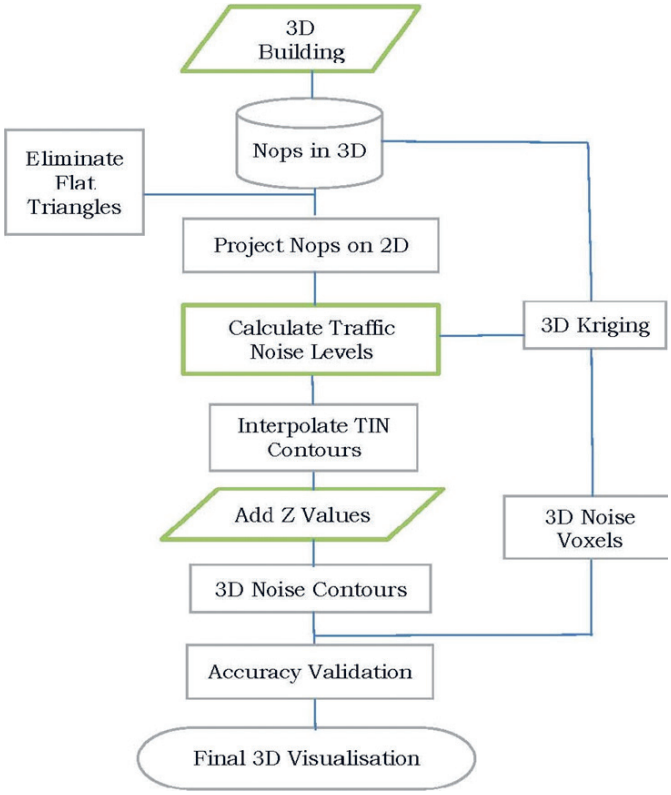

Fig. 5. Research workflow

Variations in traffic volume were not considered in this study and it was assumed that there was a continuous traffic flow. According to this study area of UTM, there is a continuous traffic flow during the morning. To increase the accuracy, numbers of vehicles were counted for fifteen working days within a three-week period and then the average number of vehicles were taken. To observe the speed of vehicles, the average speed of vehicles was observed for each type of vehicle. Ten vehicles from each category were used for this purpose. According to road traffic noise reflection, noise levels can be increased by 1.5 dB when buildings and barriers which have been located opposite side of the NOPs. $C_{\text{reflectie}}$ is the noise reflection of wall barriers and building facades. The traffic noise reflection from building facades and other hard surfaces affects the mitigation of the noise levels. Correction of noise reflection was taken as +1.5 dB [9, 66]. F_{obj} is the reflection noise on the other side of the road from the buildings and barriers, and is between 0 and 1. Only objects located at a reasonable distance will be taken to calculate noise reflection. Equation (4) shows the reflection noise from the other side of the road:

$$C_{\text{reflectie}} = 1.5F_{obj} \tag{4}$$

The noise reflection from opposite side buildings and barriers is +1.5(θ′/θ) dB, where θ is the sum of angles subtended from buildings and wall barriers. θ′ is the total angle subtended from road the segments to the receiver point [9, 66]. Figure 6 describes the traffic noise reflection correction with the building facades.

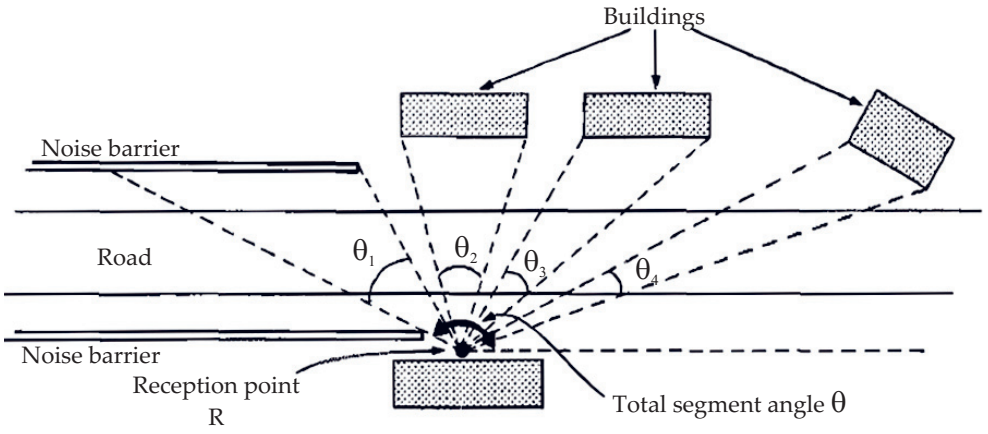

$$\text{REFLECTION CORRECTION} = +1.5\frac{\theta'}{\theta}\,\text{dB(A)}$$

where $\theta' = \theta_1 + \theta_2 + \theta_3 + \theta_4$

and θ = TOTAL SEGMENT ANGLE

Fig. 6. Noise reflection correction

Source: [66]

According to the UTM building structure, it seems that the sum of angles subtended from the opposite side buildings to a receiver point was continuous. Thus, it can be determined that the ratio of the sum of the subtended angle and the total subtended angle is 1. According to this, the noise reflection correction was taken as +1.5 dB. D_{bodem} is the traffic noise absorption by ground impact to mitigate traffic noise level [9]. Equation (5) shows the D_{bodem}:

$$D_{\text{bodem}} = B\,[2 + 4(1 - e^{-0.04r}) \cdot (e^{-0.65hw} + e^{-0.65(h\text{weg} - 0.75)})] \tag{5}$$

where:

h_{weg} – the height of the road from ground level,

h_{w} – the height of the traffic noise observation points from the reference ground level,

B – the traffic noise absorption coefficient and this is considered between the centerline of the road and the noise observation points,

r – the distance between receiver and noise source.

The value of B is between 0 and 1. This value B depends on the properties of the ground surface. For hard ground, the B is 0. The B is 1 for the areas completely covered with grass [67]. B is between 0 and 1 when the ground is covered with both hard ground and porous and B is 0.3 for gravel [68]. The ground of the study area consists of grass and hard ground. Therefore, the noise absorption coefficient of hard ground and grass was taken, respectively, to be 0 and 1. D_{meteo} represents noise reduction due to wind conditions, and it shows in Equation (6) [9]:

$$D_{meteo} = 3.5 - 3.5e^{(-0.04r/(hweg + hw + 0.75))} \quad (6)$$

where e = 2.718.

According to the equation for the reference road surface (a normal asphalt road), the surface road traffic noise correction is zero. This study area consists of a normal asphalt road. Therefore, this correction was not applied for the calculation. Furthermore, $D_{barrier}$ is the reduction of noise of wall and building barriers. There are no building and wall barriers between noise sources and receivers. Noise reduction of barriers was not considered in this study.

2.2. Developments of Data and Methods

The traffic noise decreases from 10 log r where r is the distance between the noise source and an observation point. Therefore, traffic noise reduces from approximately 1 dB within a 1 m distance [9]. Then the distance interval of NOPs was maintained 2 m in both horizontal and vertical directions (see Fig. 7). NOPs were not designed inside the buildings, due to screening noise not being considered for NOPs [24]. To avoid the issues (flat triangles) of spatial interpolation, the NOPs were designed as eliminating z coordinates with the same x and y coordinates on a vertical axis.

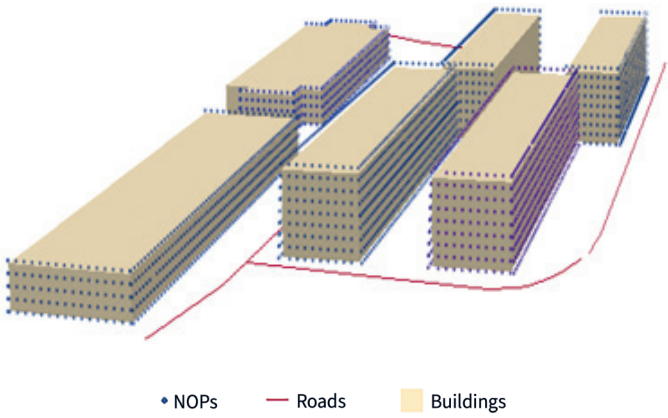

Fig. 7. Building model and NOPs

2.3. Development of Spatial Interpolation

All of these spatial interpolations, such as IDW, kriging, and TIN techniques, are used to predict the values of unknown points in the 3D space, but they have different strengths and weaknesses. Three parameters (the x coordinate, the y coordinate, and the vertical axis) can be interpolated one at a time using these interpolations [24]. However, a NOP consists of four parameters, and this means that there are two values in the vertical axis, the height of the point and the noise level. Thus, interpolating noise levels is vital along both vertical and horizontal directions. A development of 2D spatial interpolations is necessary for 3D interpolation as the 2D spatial interpolation helps to create a continuous surface in two dimensions [9]. This surface can then be used to generate a 3D interpolation. IDW, kriging, and TIN are three different types of 2D spatial interpolation methods. Designing NOPs and projecting NOPs from 3D space to 2D space is vital in development [24]. NOPs are designed along the façade of the buildings in 3D noise interpolation [26]. NOPs in the same vertical axis coincides with the same point in the 2D space, is an issue of projection. Therefore, the same x and y coordinates of z coordinates in the same vertical axis should be eliminated when designing NOPs. The distance interval with a spacing of 2 m between each NOP, and grids of NOPs, are vital in interpolation. First, interpolating the NOPs in 2D space (x coordinate, y coordinate, and noise level) is vital to generate 2D raster and vector surfaces, and 2D noise contours. Then the height values (z coordinates) for these 2D surfaces and noise contours show a 3D visualization of traffic noise mapping [24].

2.4. Development of Spatial Interpolations, Accuracy Validation, and Visualization

IDW, kriging, empirical Bayesian kriging (EBK), and TIN spatial interpolations were used to interpolate 3D noise levels. The weighting factor of IDW was selected as 2, with the number of points being 12 and the radius of the search of points being 5 m. The variogram model of kriging was considered as Gaussian, with the number of points being 12 and radius of search of points is 5 m for the interpolation. In empirical Bayesian kriging (EBK), the error of semivariogram is automatically calculated in processing time. The power variogram was used for interpolating in EBK. When considering TIN interpolation, the Delaunay triangulation method was applied for TIN interpolation. NOP consists with four parameters such x coordinate, y coordinate, z coordinate, and a noise value in a 3D space. Furthermore, IDW, kriging, EBK, and TIN do not directly support to interpolate four parameters. Therefore, a significant development should be applied to interpolate traffic noise levels in 3D. When interpolating the 3D noise levels, first all NOPs were projected in to a 2D space. It means that the z coordinate of NOP was considered as zero. The projection of 3D NOPs on the 2D space is shown in Figure 8. Then, set the TIN, IDW, kriging, and EBK surfaces to extract the noise contours. The noise contours on projected points are shown in Figure 9. Then z coordinates were inserted into the noise contours in the 2D space.

The 3D noise contours of TIN, IDW, kriging, and EBK are shown in Figures 10–13. But in 3D kriging, the projection of 3D NOPs on to 2D space is not necessary. Especially in 3D kriging, the four parameters (x, y, and z coordinates with a value) can be interpolated. In 3D kriging, the interpolated surface in 3D space shows as horizontal slices (geostatistical layers) along the vertical axis (z axis) (see Fig. 14). The voxel was created using these slices for visualizing the traffic noise (see Fig. 15). The accuracy validation of 3D noise contours (Fig. 16) and 3D noise voxels are vital for the final visualization. The root mean square error (RMSE) was used to validate the accuracy of visualization. Sound level meters (SLM) were established at corridors of the buildings. This means that SLM were established at the margin of the 1st and 2nd floors and the margin of the 2nd and 3rd floors. A DEKKO SL-130, sound level meter was used. The accuracy of this noise meter is ±0.1 dB and noise levels were observed at twenty locations. The noise levels were observed when perpendicular propagation from the centerline of the road to the receiver. Noise levels were observed for fifteen days, in the morning from 7.30 a.m. to 9.30 a.m., and average noise levels were taken for the twenty locations. Then, the corresponding noise levels of twenty locations with 3D voxel value and 3D noise contour value was considered for the accuracy validation. The RMSE value was calculated for 3D noise contours and 3D noise voxels.

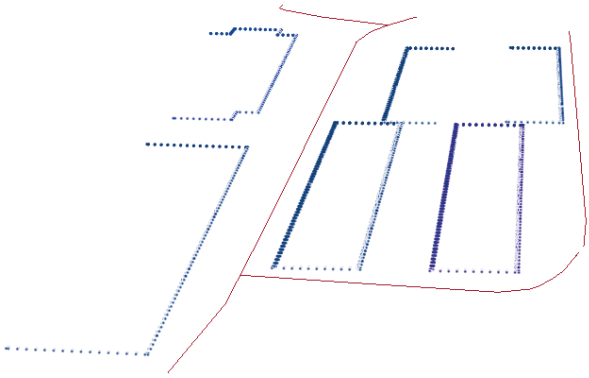

Fig. 8. Projection of NOPs on 2D space

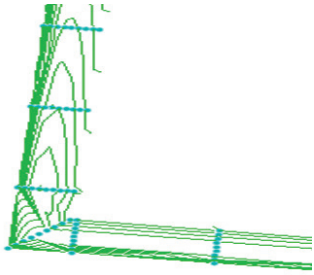

Fig. 9. Noise contours and projected NOPs

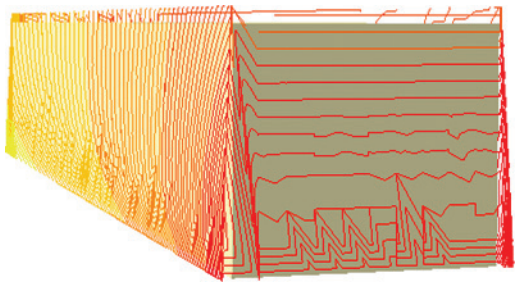

Fig. 10. TIN noise contours

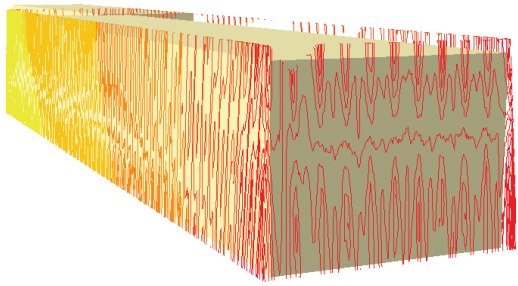

Fig. 11. IDW noise contours

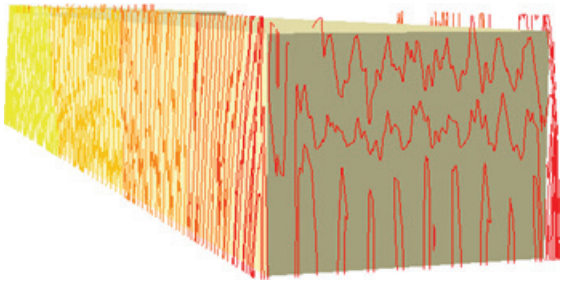

Fig. 12. Kriging noise contours

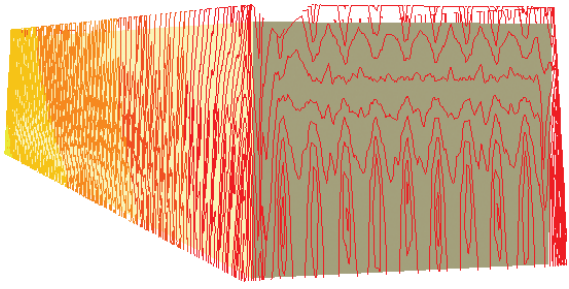

Fig. 13. EBK noise contours

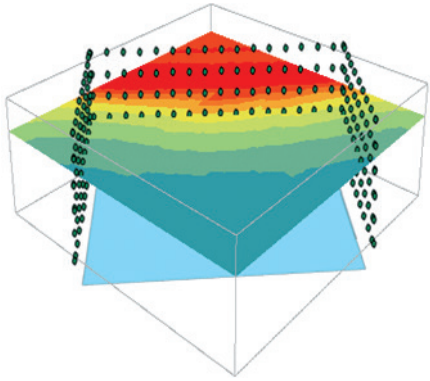

Fig. 14. 3D kriging slices

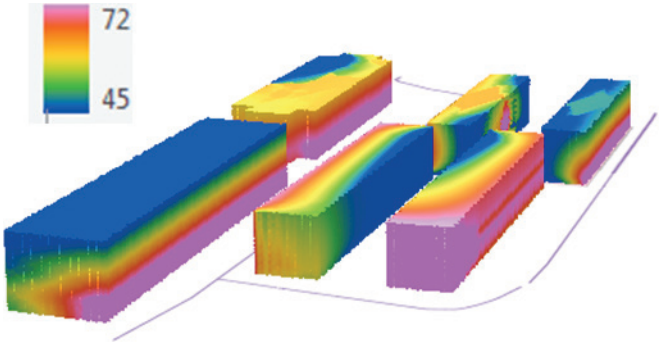

Fig. 15. 3D kriging voxel noise model

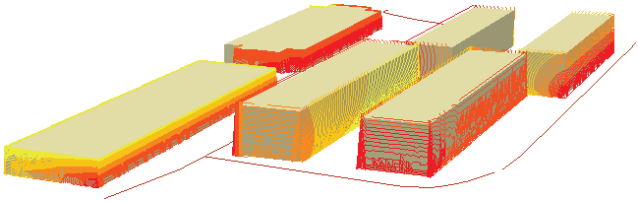

Fig. 16. Model of TIN noise contours

3. Results and Discussion

3D contours and voxels are vital for road traffic noise visualization. In this investigation, road traffic noise was embedded with a 3D building model. Complex and simple building models are widely used for the applications of environmental managements. The simple building model is sufficient to visualize the traffic noise levels due to the road traffic noise reducing approximately 1 dB for 2 m during the

propagation. According to this theory of road traffic noise, the 2 m distance was managed while designing NOPs in both horizontal and vertical axis. Road traffic noise levels change more slowly in the same horizontal levels than in the vertical direction. According to the Henk de Kluijver noise equation, the noise reflection by buildings of opposite sides and noise absorption by ground effect to change the traffic noise levels in same horizontal level. According to the model of 3D voxel road traffic noise visualization and 3D road traffic noise contours, the decreasing road traffic noise levels is higher from ground level to the 1st floor than from the 1st floor to the 2nd floor. According to the Henk de Kluijver road traffic model, this is because of traffic noise absorption by the ground and reflection. If the noise source is a point source, the noise decreases by 6 dB with the doubling of the distance. If the noise source is a line source, there is no such noise reduction with the doubling of the distance. If there is a busy (continuous traffic flow), it may be considered as line source. In this study area, there was a higher continuous traffic flow during 7.30 a.m. to 9.30 a.m. Therefore, road traffic noise sources are considered as line sources in this study.

The distance between NOPs and vehicles affect changing road traffic noise levels in the vertical direction by means of the above-mentioned absorption and reflection. The RMSE was considered for the validation of the TIN noise contours and the 3D kriging voxels visualization. Twenty sample of noise observation points were collected in the corridors of the buildings. This means that the validation of road traffic noise was only conducted along the facades of the buildings. Two noise meters were used to collect noise observations and thus, all observation samples of the same vertical direction along building facades were taken at the same time. This means that, sound level meters were located along same vertical direction at the margin of 1st floor and 2nd floor and 2nd floor to 3rd floor, a technique used to improve the accuracy of sample points. Because the road traffic noise levels were considered outside of the facades of buildings, the road traffic noise levels inside the buildings were not considered. If the influence of building materials on road traffic noise propagation were considered, the road traffic noise levels inside the buildings can be calculated and this will be a main significant development of this study in the future.

The RMSE for TIN noise contours was 1.114, and it was 0.726 for the visualization of 3D kriging voxels. The IDW, kriging, and EBK noise contours were not considered for the accuracy validation, and those contours were the irregular shapes. The noise contour was 0.2 dB. The noise levels were changed approximately 0.2 dB at NOPs in the same vertical direction. In that sense, the difference between the values of NOPs (calculated noise levels) and the values of predictions (interpolated values) is small. The weighting factor of IDW denotes the significance of the predicted values and the calculated values. When the weighting factor increases, the similarity between the calculated and interpolated values also increases. Therefore, the unpredictable oscillations are in interpolated values. According to the results of these irregular IDW contours, it can be concluded that the value difference of NOPs was not matched with the power factor of IDW that was used in this study. However,

it is not possible to use the weighting factor that is below 2 because the function of IDW is polynomial. Due to the small difference of NOP values, it seems that there is correlation between NOPs and thus they are considered as clusters for kriging and EBK interpolation. Therefore, this may be the reason for irregular noise contours. Moreover, the value for the prediction is taken from neighboring points in IDW, kriging, and EBK. However, only one nearest point is considered in the TIN interpolation, serving as a motivation to obtain nonirregular noise contours from TIN. The visualization of the TIN noise contours is shown in Figure 14. However, there are irregular shape contours at the ground level. It seems that it is not possible to use the Henk de Kluijver noise model to calculate noise levels at ground level but the noise contours have regular shapes at 1 m from ground level.

The 3D kriging provides a significant approach in interpolating traffic noise levels in a 3D space. The 3D geostatistical layers are created along the vertical axis in 3D kriging. The sample model of the 3D geostatistical layer of 3D kriging of this study is illustrated in Figure 15. The distance interval of NOPs at 2 m was used and the variogram was selected as the power for 3D kriging interpolation. If there is an accuracy comparison among all the variograms in 3D kriging, it is a better solution for the final traffic noise visualization. After creating 3D geostatistical layers, 3D voxels were used to visualize traffic noise in raster format. According to variations in traffic noise levels at NOPs, the height of the voxel was taken as 0.1 m and the length was 0.5 m, and width was 0.5 m. The road traffic noise visualisation of the 3D voxels is shown in Figure 16.

4. Conclusions

Road traffic noise visualization in 3D is important for both developed and developing cities and identifying a suitable road traffic noise model is vital to accurately calculate noise levels. According to the accuracy of the visualization of road traffic noise levels, the Henk de Kluijver traffic model can be suggested for the calculation of road traffic noise levels along a vertical direction. When road traffic noise propagates over the ground, noise energy will be lost by absorption. According to the Henk de Kluijver road traffic noise model, traffic noise absorption by the ground depends on the noise absorption coefficient of the ground, the height of the noise source, and the receiver height. Thus, if there are no noise barriers and topography undulations, the receiver noise levels are not changed. Then, traffic noise levels are the same for the same horizontal lines from the centerline. However, when considering road traffic noise propagation along the vertical direction, receiver heights are changed along the same vertical direction. Therefore, road traffic noise levels change along the vertical direction. This study was conducted to visualize road traffic noise levels on the outer facades of buildings only. Thus, the acoustic insulation of building materials was not considered. Therefore, road traffic noise levels were

not visualized inside the buildings. However, if the acoustic insulation properties of building materials used in windows, doors, roofs, and walls (bricks, cement, or wood) can be determined, this research can also be developed to visualize road traffic noise levels inside buildings.

Designing NOPs and spatial interpolation is vital for the visualization of traffic noise. Ideally, flat triangles (different z values for the same x and y coordinates) should be eliminated along the vertical direction while designing NOPs. The distance interval of a pair of NOPs depends on the parameters of the traffic noise model. Designing NOPs on grids involve improving the accuracy of interpolated surface. The noise contours and noise voxels are the keys to visualize traffic noise. However, the developments of the data and spatial interpolation should be applied for traffic noise visualization. NOP is a 3D space having four parameters such as the x coordinate, the y coordinate, the z coordinate and the noise level. But IDW, kriging, EBK and TIN spatial interpolations are not directly supported to interpolate four parameters. Therefore, the NOPs that are in a 3D space should be projected onto a 2D space. After the interpolation has been done, the height value (z coordinates) can be inserted. However, the noise contours of IDW, kriging, and EBK provide irregular shapes of the contours. The 3D kriging provides significance approaches to interpolate four parameters. The processing of 3D kriging geostatistical layers into voxels is of primary importance for visualizing traffic noise in voxels. Furthermore, the noise visualization by 3D voxels shows higher accuracy than TIN noise contours. However, this study could be developed to visualize road traffic noise using voxel contours in the future.

Author Contributions

Nevil Wickramathilaka: conceptualization and identification, methodology, software, design analysis, model, writing, 3D visualization and validation.

Uznir Ujang: supervision, conceptualization, research gap investigation, validation, review and editing, project administration, funding acquisition.

Suhaibah Azri: supervision, writing – review and editing, project administration, funding acquisition.

Tan Liat Choon: supervision, review and editing, funding acquisition.

Acknowledgements

This research was conducted according to the requirements and guidance of the 3D GIS Research Lab at Universiti Teknologi Malaysia.

References

[1] Iglesias-Merchan C., Laborda-Somolinos R., González-Ávila S., Elena-Rosselló R.: *Spatio-temporal changes of road traffic noise pollution at eco-regional scale*. Environmental Pollution, vol. 286, 2021, 117291. https://doi.org/10.1016/j.envpol.2021.117291.

[2] Subramani T., Kavitha M., Sivaraj K.P.: *Modelling of traffic noise pollution*. International Journal of Engineering Research and Application, vol. 2(3), 2012, pp. 3175–3182. https://www.ijera.com/papers/Vol2_issue3/TB2331753182.pdf [access: 11.06.2023].

[3] Majid M., Abid R., Ali A., Ahmad S.: *Physiological and psychological impacts of noise pollution on the workers; a case study in Textile Mills of Multan Pakistan*. Pakistan Journal of Science, vol. 73(2), 2021, pp. 397–402. https://pjosr.com/index.php/pjs/article/view/677/185 [access: 11.06.2023].

[4] Rahmani S., Mousavi S.M., Kamali M.J.: *Modeling of road-traffic noise with the use of genetic algorithm.* Applied Soft Computing, vol. 11(1), 2011, pp. 1008–1013. https://doi.org/10.1016/j.asoc.2010.01.022.

[5] Salomons E.M., Zhou H., Lohman W.J.: *Efficient numerical modeling of traffic noise*. Journal of the Acoustical Society of America, vol. 127(2), 2010, pp. 796–803. https://doi.org/10.1121/1.3273890.

[6] Monazzam M.R., Karimi E., Shahbazi H., Shahidzadeh H.: *Effect of cycling development as a non-motorized transport on reducing air and noise pollution-case study: Central districts of Tehran.* Urban Climate, vol. 38, 2021, 100887. https://doi.org/10.1016/j.uclim.2021.100887.

[7] Butler D.: *Noise management: Sound and vision*, vol. 427, 2004, pp. 480–481. https://doi.org/10.1038/427480a.

[8] Lee H.M., Luo W., Xie J., Lee H.P.: *Traffic noise reduction strategy in a large city and an analysis of its effect.* Applied Sciences, vol. 12(12), 2022, 6027. https://doi.org/10.3390/app12126027.

[9] Ranjbar H.R., Gharagozlou A.R., Vafaei Nejad A.R.: *3D analysis and investigation of traffic noise impact from Hemmat Highway located in Tehran on buildings and surrounding areas.* Journal of Geographic Information System, vol. 4(4), 2012, pp. 322–334. https://doi.org/10.4236/jgis.2012.44037.

[10] Mishra R.K., Mishra A.R., Singh A.: *Traffic noise analysis using RLS-90 model in urban city.* [in:] *Noise control for a better environment: Proceedings of the 48th International Congress and Exhibition on Noise Control Engineering INTERNOISE 2019, Madrid, June 16–19, 2019*, vol. 13, 2019, pp. 6490–6502.

[11] Dubey R., Bharadwaj S., Sharma V.B., Bhatt A., Biswas S.: *Smartphone-based traffic noise mapping system.* International Archives of the Photogrammetry, Remote Sensing and Spatial Information Sciences, vol. XLIII-B4, 2022, pp. 613–620. https://doi.org/10.5194/isprs-archives-XLIII-B4-2022-613-2022.

[12] Dipeshkumar R.S., Bhaven N.T.: *A review on GIS-based approach for road traffic noise mapping.* Indian Journal of Science and Technology, vol. 12(14), 2019, pp. 1–6. https://doi.org/10.17485/ijst/2019/v12i14/132481.

[13] Adza W.K., Hursthouse A.S., Miller J., Boakye D.: *Exploring the combined association between road traffic noise and air quality using QGIS*. International Journal of Environmental Research and Public Health, vol. 19(24), 2022, 17057. https://doi.org/10.3390/ijerph192417057.

[14] Gozalo R.G., Suárez E., Montenegro A.L., Arenas J.P., Morillas Barrigón J.M., Montes González D.: *Noise estimation using road and urban features*. Sustainability, vol. 12(21), 2020, 9217. https://doi.org/10.3390/su12219217.

[15] Ranpise R.B., Tandel B.N., Singh V.A.: *Development of traffic noise prediction model for major arterial roads of tier-II city of India (Surat) using artificial neural network.* Noise Mapping, vol. 8(1), 2021, pp. 172–184. https://doi.org/10.1515/noise-2021-0013.

[16] Adulaimi A.A.A., Pradhan B., Chakraborty S., Alamri A.: *Traffic noise modelling using land use regression model based on machine learning, statistical regression and GIS*. Energies, vol. 14(16), 2021, 5095. https://doi.org/10.3390/en14165095.

[17] Islam Z., Abdullah F., Khanom M.: *Evaluation of traffic accessibility condition and noise pollution in Dhaka City of Bangladesh*. American Journal of Traffic and Transportation Engineering, vol. 6(2), 2021, pp. 43–51. https://doi.org/10.11648/j.ajtte.20210602.12.

[18] Malherbe M., McIntyre T., Hattingh T.V., Leresche P.M., Haussmann N.S.: *Mammal road-type associations in Kruger National Park, South Africa: Common mammals do not avoid tar roads more than dirt roads.* Ecology and Evolution, vol. 11(12), 2021, pp. 15622–15629. https://doi.org/10.1002/ece3.8190.

[19] Seong J.C., Park T.H., Ko J.H., Chang S.I., Kim M., Holt J.B., Mehdi M.R.: *Modeling of road traffic noise and estimated human exposure in Fulton County, Georgia, USA*. Environment International, vol. 37(8), 2011, pp. 1336–1341. https://doi.org/10.1016/j.envint.2011.05.019.

[20] Sabillon C., Hernandez J., Li R., Huang., Prozzi J.A.: *Efficient Model for Predicting Friction on Texas Highway Network. Technical Report 0-7031-1*. The University of Texas at Austin, Center for Transportation Research, Austin, TH, USA, 2023. https://rosap.ntl.bts.gov/view/dot/66238 [access: 11.06.2023].

[21] Quartieri J., Mastorakis N.E., Iannone G., Guarnaccia C., D'Ambrosio S., Troisi A., Lenza T.L.L.: *A review of traffic noise predictive noise models*. Recent Advances in Applied and Theoretical Mechanics, 2009, pp. 72–80.

[22] Zafar M.I., Dubey R., Bharadwaj S., Kumar A., Paswan K.K., Srivastava A., Tiwary S.K., Biswas S.: *GIS based road traffic noise mapping and assessment of health hazards for a developing urban intersection*. Acoustics, vol. 5(1), 2023, pp. 87–119. https://doi.org/10.3390/acoustics5010006.

[23] Rajakumara H.N., Gowda R.M.M.: *Road traffic noise prediction models: a review*. International Journal of Sustainable Development and Planning, vol. 3(3), 2008, pp. 257–271. https://doi.org/10.2495/SDP-V3-N3-257-271.

[24] Kurakula V.K., Kuffer M.: *3D noise modeling for urban environmental planning and management.* [in:] Schrenk M., Popovich V.V., Engelke D., Elisei-real P. (eds.), *CORP 008: Mobility Nodes as Innovation Hubs: Proceedings of 13th International Conference on Urban Planning, Regional Development and Information Society, Vienna, May 19–21 2008*, Competence Center of Urban and Regional Planning, Schwechat 2008, pp. 517–523.

[25] Huang B., Pan Z., Liu Z., Hou G., Yang H.: *Acoustic amenity analysis for high-rise building along urban expressway: Modeling traffic noise vertical propagation using neural networks.* Transportation Research. Part D: Transport and Environment, vol. 53, 2017, pp. 63–77. https://doi.org/10.1016/j.trd.2017.04.001.

[26] Lu L., Becker T., Löwner M.-O.: *3D Complete Traffic Noise Analysis Based on CityGML*. [in:] Abdul-Rahman A. (ed.), *Advances in 3D Geoinformation*, Lecture Notes in Geoinformation and Cartography, Springer, Cham 2017, pp. 265–283. https://doi.org/10.1007/978-3-319-25691-7_15.

[27] Puyana-Romero V., Cueto J.L., Gey R.: *A 3D GIS tool for the detection of noise hot-spots from major roads*. Transportation Research. Part D: Transport and Environment, vol. 84, 2020, 102376. https://doi.org/10.1016/j.trd.2020.102376.

[28] Li J., Heap A.D.: *Spatial interpolation methods applied in the environmental sciences: A review*. Environmental Modelling and Software, vol. 53, 2014, pp. 173–189. https://doi.org/10.1016/j.envsoft.2013.12.008.

[29] Hu Q., Li Z., Wang L., Huang, Wang Y., Li L.: *Rainfall spatial estimations: A review from spatial interpolation to multi-source data merging*. Water, vol. 11(3), 2019, 579. https://doi.org/10.3390/w11030579.

[30] Jiang Q., Peng J., Biswas A., Hu J., Zhao R., He K., Shi Z.: *Characterising dryland salinity in three dimensions*. Science of the Total Environment, vol. 682, 2019, pp. 190–199. https://doi.org/10.1016/j.scitotenv.2019.05.037.

[31] Harman B.I., Koseoglu H., Yigit C.O.: *Performance evaluation of IDW, Kriging and multiquadric interpolation methods in producing noise mapping: A case study at the city of Isparta, Turkey*. Applied Acoustics, vol. 112, 2016, pp. 147–157. https://doi.org/10.1016/j.apacoust.2016.05.024.

[32] Che D., Jia Q.: *Three-dimensional geological modeling of coal seams using weighted Kriging method and multi-Source data.* IEEE Access, vol. 7, 2019, pp. 118037–118045. https://doi.org/10.1109/Access.2019.2936811.

[33] Comber A., Zeng W.: *Spatial interpolation using areal features: A review of methods and opportunities using new forms of data with coded illustrations.* Geography Compass, vol. 13(10), 2019, e12465. https://doi.org/10.1111/gec3.12465.

[34] Laxmi V., Dey J., Kalawapudi K., Vijay R., Kumar R.: *An innovative approach of urban noise monitoring using cycle in Nagpur, India*. Environmental Science and Pollution Research, vol. 26, 2019, pp. 36812–36819. https://doi.org/10.1007/s11356-019-06817-0.

[35] Alcaras E., Amoroso P.P., Parente C.: *The influence of interpolated point location and density on 3D bathymetric models generated by kriging methods: An application on the Giglio Island Seabed (Italy).* Geosciences, vol. 12(2), 2022, 62. https://doi.org/10.3390/geosciences12020062.

[36] Maiti P., Mitra D.: *Ordinary kriging interpolation for indoor 3D REM.* Journal of Ambient Intelligence and Humanized Computing, 2022, pp. 1–15. https://doi.org/10.1007/s12652-022-03784-2.

[37] He L., Zhang J., Chen S., Hou M., Chen J.: *Three-dimensional hydrogeological modeling method and application based on TIN-GTP-TEN*. Earth Science Informatics, vol. 15(1), 2022, pp. 337–350. https://doi.org/10.1007/s12145-021-00727-x.

[38] Tomczak M.: *Spatial interpolation and its uncertainty using automated anisotropic Inverse Distance Weighting (IDW)-Cross-validation/Jackknife Approach.* Journal of Geographic Information and Decision Analysis, vol. 2(2), 1998, pp. 18–30.

[39] Samal K.K.R., Babu K.S., Das S.K.: *Spatio-temporal prediction of air quality using distance-based interpolation and deep learning techniques*. EAI Endorsed Transactions on Smart Cities, vol. 5(14), 2021,168139. https://doi.org/10.4108/eai.15-1-2021.168139.

[40] Schneck T., Telbisz T., Zsuffa I.: *Precipitation interpolation using digital terrain model and multivariate regression in hilly and low mountainous areas of Hungary.* Hungarian Geographical Bulletin, vol. 70(1), 2021, pp. 35–48. https://doi.org/10.15201/hungeobull.70.1.3.

[41] Neissi L., Golabi M., Gorman J.M.: *Spatial interpolation of sodium absorption ratio: A study combining a decision tree model and GIS*. Ecological Indicators, vol. 117, 2020, 106611. https://doi.org/10.1016/j.ecolind.2020.106611.

[42] Purnomo H.: *A practical application of Inverse Distance Weighting method to identify cobalt anomaly distribution in Laterite Deposit (Case study in Block R, Wasile Subdistrict, East Halmahera*. [in:] Prastowo R., Nurdiyanto H. (eds.), *ICITID 2021: Proceedings of the 2nd International Conference on Industrial and Technology and Information Design, 30 August 2021, Yogyakarta, Indonesia*, EAI, 2021. https://doi.org/10.4108/eai.30-8-2021.2311529.

[43] Varentsov M., Esau I., Wolf T.: *High-resolution temperature mapping by geostatistical kriging with external drift from large-eddy simulations*. Monthly Weather Review, vol. 148(3), 2020, pp. 1029–1048. https://doi.org/10.1175/MWR-D-19-0196.1.

[44] Fung K.F., Chew K.S., Huang Y.F., Ahmed A.N., Teo F.Y., Ng J.L., Elshafie A.: *Evaluation of spatial interpolation methods and spatiotemporal modeling of rainfall distribution in Peninsular Malaysia.* Ain Shams Engineering Journal, vol. 13(2), 2022, 101571. https://doi.org/10.1016/j.asej.2021.09.001.

[45] Debnath A., Singh P.K.: *Environmental traffic noise modelling of Dhanbad township area – A mathematical based approach*. Applied Acoustics, vol. 129, 2018, pp. 161–172. https://doi.org/10.1016/j.apacoust.2017.07.023.

[46] Maleika W.: *Inverse distance weighting method optimization in the process of digital terrain model creation based on data collected from a multibeam echosounder*. Applied Geomatics, vol. 12(4), 2020, pp. 397–407. https://doi.org/10.1007/s12518-020-00307-6.

[47] Aumond P., Can A., Mallet V., De Coensel B., Ribeiro C., Botteldooren D., Lavandier C.: *Kriging-based spatial interpolation from measurements for sound level mapping in urban areas*. The Journal of the Acoustical Society of America, vol. 143(5), 2018, pp. 2847–2857. https://doi.org/10.1121/1.5034799.

[48] Lesieur A., Mallet V., Aumond P., Can A.: *Data assimilation for urban noise mapping with a meta-model.* Applied Acoustics, vol. 178, 2021, 107938. https://doi.org/10.1016/j.apacoust.2021.107938.

[49] van Groenigen J.W.: *The influence of variogram parameters on optimal sampling schemes for mapping by kriging*. Geoderma, vol. 97(3–4), 2000, pp. 223–236. https://doi.org/10.1016/S0016-7061(00)00040-9.

[50] Ramadhan M.D., Marwanza I., Nas C., Azizi M.A., Dahani W., Kurniawati R.: *Drill holes spacing analysis for estimation and classification of coal resources based on variogram and kriging*. IOP Conference Series: Earth and Environmental Science, vol. 819(1), 2021, 012026. https://doi.org/10.1088/1755-1315/819/1/012026.

[51] Jaman N.I. Adhikary S.K.: *A positive kriging approach for missing rainfall estimation*. [in:] *ICCESD 2020: Proceedings of the 5th International Conference on Civil Engineering for Sustainable Development, 7–9 February 2020, KUET, Khulna, Bangladesh*, 2020.

[52] Wenzhong S.: *Development of a hybrid model for three-dimensional GIS*. Geo-Spatial Information Science, vol. 3(2), 2000, pp. 6–12.

[53] Zelt C.A., Azaria A., Levander A.: *3D seismic refraction traveltime tomography at a groundwater contamination site*. Geophysics, vol. 71(5), 2006, pp. H67–H78. https://doi.org/10.1190/1.2258094.

[54] Hammad A.W.A., Akbarnezhad A., Rey D.: *A multi-objective mixed integer nonlinear programming model for construction site layout planning to minimise noise pollution and transport costs*. Automation in Construction, vol. 61, 2016, pp. 73–85. https://doi.org/10.1016/j.autcon.2015.10.010.

[55] Venkataraman S., Asante K.O.: *Voxel-based analysis and visualization of rainfall data*. [in:] *Pecora 16 "Global Priorities in Land Remote Sensing", October 23–27, 2005, Sioux Falls, South Dakota 2005*.

[56] Grunwald S., Barak P., Rooney D.*: Web-based virtual models for the Earth Science Community*. [in:] *ASAE International Meeting in Sacramento, CA, July 29–August 1, 2001*, American Society of Agricultural Engineers, 2001, pp. 1–9.

[57] *What is Empirical Bayesian Kriging 3D?* ESRI, 2020. https://pro.arcgis.com/en/proapp/latest/help/analysis/geostatistical-analyst/what-is-empirical-bayesian-kriging-3d-.htm [access: 11.06.2023].

[58] Zhang Y., Ji W., Saurette D.D., Easher T.H., Li H., Shi Z., Adamchuk V.I., Biswas A.: *Three-dimensional digital soil mapping of multiple soil properties at a field-scale using regression kriging.* Geoderma, vol. 366, 2020, 114253. https://doi.org/10.1016/j.geoderma.2020.114253.

[59] Chen C., Hu K., Li H., Yun A., Li B.: *Three-dimensional mapping of soil organic carbon by combining kriging method with profile depth function*. PLoS ONE, vol. 10(6), 2015, e0129038. https://doi.org/10.1371/journal.pone.0129038.

[60] Sukkuea A., Heednacram A.: *Prediction on spatial elevation using improved kriging algorithms: An application in environmental management.* Expert Systems with Applications, vol. 207, 2022, 117971. https://doi.org/10.1016/j.eswa.2022.117971.

[61] Izady A., Abdalla O., Ahmadi T., Chen M.: *An efficient methodology to design optimal groundwater level monitoring network in Al-Buraimi region, Oman.* Arabian Journal of Geosciences, vol. 10(2), 2017, 26. https://doi.org/10.1007/s12517-016-2802-2.

[62] Xu Y., Tong X., Stilla U.: *Voxel-based representation of 3D point clouds: Methods, applications, and its potential use in the construction industry.* Automation in Construction, vol. 126. 2021, 103675. https://doi.org/10.1016/j.autcon.2021.103675.

[63] Saglam A., Makineci H.B., Baykan N.A., Baykan Ö.K.: *Boundary constrained voxel segmentation for 3D point clouds using local geometric differences*. Expert Systems with Applications, vol. 157, 2020, 113439. https://doi.org/10.1016/j.eswa.2020.113439.

[64] Wu H., Zhu Q., Guo Y., Zheng W., Zhang L., Wang Q., Zhou R., Ding Y., Wang W., Pirasteh S., Liu M.: *Multi-level voxel representations for digital twin models of tunnel geological environment*. International Journal of Applied Earth Observation and Geoinformation, vol. 112, 2022, 102887. https://doi.org/10.1016/j.jag.2022.102887.

[65] Li J., Liu P., Wang X., Cui H., Ma Y.: *3D geological implicit modeling method of regular voxel splitting based on layered interpolation data.* Scientific Reports, vol. 12(1), 2022, 13840. https://doi.org/10.1038/s41598-022-17231-x.

[66] Hood R.A.: *Accuracy of calculation of road traffic noise*. Applied Acoustics, vol. 21(2), 1987 pp. 139–146. https://doi.org/10.1016/0003-682X(87)90006-5.

[67] ISO 9613-2:1996: *Acoustics – Attenuation of sound during propagation outdoors – Part 2: General method of calculation*.

[68] Attenborough K., Bashir I., Taherzadeh S.: *Exploiting ground effects for surface transport noise abatement.* Noise Mapping, vol. 3(1), 2016, pp. 1–25. https://doi.org/10.1515/noise-2016-0001.